Exploring Control Design of a PV-Wind Hybrid On-Grid System without ESD

[1]Ramesh Chander Bansal, [2] Alok Kumar Bharadwaj

[1]PhD Scholar,[2] Professor
[1,2]Electrical Engineering Department, Mewar University, Rajasthan, India.

***Abstract*—there is general practice to support and compensate intermittent behavior of Solar photovoltaic (PV) system with energy storage devices (ESD) and the one generally adopted is battery energy storage (BES) simply because of lower cost as compared to fuel cells or a bank of super capacitors. However, cost of battery maintenance, inherent shorter life, even if state of charge (SOC) is regulated; involving comparatively huge capital investment is a big issue. In this paper, a stabilized hybrid photovoltaic-wind grid connected system without battery storage or ESD is developed with effective and co-ordinate control of current injection into grid with maximized harvest of PV energy using MPPT control and wind energy transfer control automatically. The control philosophy of energy transfer to PCC is an algebraic sum of energy using MPPT of PV system in relation to inverter stage while that of wind system is through wind converter. The stability mechanism of battery or ESD supported system, is getting replaced by a mechanism of current injection to grid by sharing both components of hybrid renewable sources. This is simulated in MATLAB/ Simulink to validate the effectiveness of proposed system.**

***Index Terms*—Coordinated Current injection control, Hybrid grid, Grid connected photovoltaic, Maximum Power Point Tracking (MPPT), Renewable energy, Photovoltaic system, Wind energy.**

I. INTRODUCTION

We all are aware about terms like ecosystem, fossil fuel limitations, global warming, glaciers melting, co2 layer decreasing and there is increasing concern about use of Sun, Wind, water, natural gas and other natural resources on which our future will be depending to meet increasing energy demands.Further there is growing preference for distributed grids and micro-grids with majority of renewable sources like PV, wind energy storage devices (ESD) and DG sets. Being environmental resources their behavior is changing, not fully predictable and needs costly ESD.PV arrays, wind turbines, fuel cells, micro turbines, conventional diesel and natural gas reciprocating engines, gas-fired turbines, steam turbines, and energy storage technologies are some of the basic distributed resources(DR).

Theoretically concept of grid is good but practical implementations faces challenges with renewable resources integration for their power capacity share optimization and refinement as stable, sustainable with reliability of supply in all times of metrological changes in environment.The PV arrays are joined in arrays with various series-parallel combinations to achieve targeted voltage and current ratings as well ensuring power conversion at the maximum power point tracking (MPPT) [2-7].In case there is higher current requirement the parallel combinations are increased with implementations of distributed MPPT (DMPT) which is a better and natural choice to take care of shadowing effect. Normally there are two power converters in a two stage PV system [8-9]. In a two stage PV system, a dc-dc converter with boost action is introduced to stabilize common dc bus acting as a source to DC-AC converter or an central inverter with outgoing filter to arrest DC component and high frequency harmonics before hooking up to a point of common coupling (PCC) at grid. Alternately the array inverters are synchronized in AC form at PCC.

In case of wind energy, the differential pressure generated by the wind flowing through the wind turbine, rotate the power generator to generate electricity. With the optimal power tracking technique, the wind turbine output power can be kept at the maximum power operating point. Then, the output is converted into DC power through a rectifier. Using a voltage step-up circuit, the converted high-voltage DC power is sent to the inverter before entering the transformer to convert the DC power into AC power

The interaction of DR with electrical power system (EPS) depends upon its form and type of associated electric converter such as synchronous, asynchronous (induction generator) or a static electronic converter with designed topology. The system as a whole responds differently because of varying electrical and mechanical inertia and response times of the control system. A synchronous generator running at synchronous shaft speed is directly synchronized with EPS supplying real power as per governor of prime mover and reactive power as per excitation of the field; while induction generator is not in synchronism and its rotational speed varies with prime mover but to transfer energy into EPS they are supposed to rotate slightly higher at synchronized speed.However the static converter provides parametric matching with EPS and ensure a grid synchronizing within

safety bound limits. Synchronous machine control is complex and also need special protection equipment under fault condition but supports power factor improvement of EPS. Induction machine always absorbs reactive power with deteriorated power factor. High speed reliable comparators are utilized for automatic synchronization and complying with IEEE 1547-2003 requirements resulting reduced risk and impact on the equipments. The abnormal issues in the interconnected DR may arise:

- High or low battery or array voltage
- High or low utility line voltage
- Loss of utility
- Momentary transients and EMI noise
- Phase unbalance and induced dc transients
- Resonance and oscillation at start and switching of the DR loads
- Break in synchronization
- Rise in temperature and overload of equipment

In case of off grid system, the local resources, loads and ESD^s are to be coordinated not only for meeting day and night loads but also category wise normal and emergency loads.

Battery supported ongrid as well off grid renewable hybrid systems are in practice despite of partly justified higher capital investment and shorter life. There are reports in the literature to maintain the SOC of battery and thereby enhancing its life but it may considered as better state of utilization with reduced cost burden and certainly not a problem resolution. In this paper possibility of battery elimination or reducing the required capacity is studied in the proposed hybrid PV-wind power system which may be on or off grid system.

II. Description of Considered Grid Connected System

In the proposed PV-wind hybrid grid connected system, 12 PV modules are connected in series to form a string and 66 such strings are connected in parallel to fulfill the current and voltage needs of the system. PV modules are connected to the grid through 3-phase inverter via EMI filter; forming a single stage PV system. To ensure maximum extraction of PV power Perturb & Observe (P&O) based MPPT control is implemented on 3-phase inverter or in other words inverter control is taking care of power injection to the grid. Wind generator is connected to the point of common coupling (PCC) as depicted in Fig. 1. Grid side controller and rotor side controller are taking care of wind energy being transferred to the grid. In designed PV-wind hybrid grid system the share of PV power is 152 kW and that of wind generator power is 80 kW and thus total system capacity is 232 kW. PV module specifications are presented in Table I. Further wind turbine specifications with same cut-out speed are grouped in Table II. Depending upon the voltage level of power being generated by PV-wind system, step up transformer is calculated. In considered case, step up transformer is required to match the voltage level of utility grid as per designed PV-wind generating system.

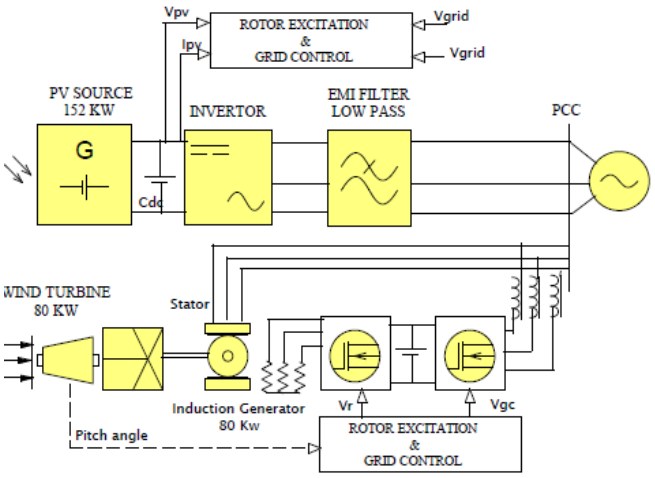

Fig. 1 Block diagram of proposed PV-wind hybrid grid connected system

TABLE I. Specification of each module

Maximum power, P_{mppt} (W)	305
Voltage at MPP, V_{mppt}(V)	54.7
Open circuit voltage V_{oc} (V)	64.2
Current at MPP, I_{mppt} (A)	5.58
Short circuit current, I_{sc} (A)	5.96
Number of PV cells connected in series, N_s	96
Series resistance, R_S (Ω)	0.037998
Parallel resistance, R_P (Ω)	993.51
Saturation current, I_{sat} (μA)	0.011753
PV unit power (W)	610
PV unit V_{mppt} (V)	54.7*2
PV unit I_{mppt} (A)	5.58

TABLE II. Specification of Wind Turbine with same cut-out speed

S no.	Turbine Model	Power rating Mw	Speed rating m/sec	Cut-in Speed m/sec	Cut-out Speed m/sec
1	Vestas V-52	0.85	16	4	25
2	Sulzon S-88	2.1	14	4	25
3	W1250	1.25	12	4	25
4	Norwin 150	0.2	12.5	4	25
5	Gamesa G66	1.65	15	4	25

A. PV system mathemetical model and implementation

The modules in a PV system are typically connected in arrays with series and parallel configurations. Electrical modeling of suggested PV array system is represented in the following equations [1]:

$$V_{pv} = \left(\frac{B \times K \times T \times N_s}{q}\right) \times \ln\left(\frac{N_p\,(I_L + I_{os} - I_{pv})}{N_p \times I_{os}}\right) \quad (1)$$

$$I_{os} = I_{or}\left[\frac{T}{T_r}\right]^3 \exp\left(\frac{q\,E_{Go}}{BK}\left(\frac{1}{T_r} - \frac{1}{T}\right)\right) \quad (2)$$

$$T_c = T_{air} + 0.2 \times H\% \quad (3)$$

Where, V_{pv} is the PV array output voltage, I_{pv} is the PV array output current, I_{or} is the reverse saturation current, I_{os} is the cell reverse saturation current (A), N_s is the number of cells connected in series, N_p is the number of cells connected in parallel, I_L is the light generated current (A), B is the ideality factors , K is the Boltzmann's constant, q is the electronic charge, T_r is the reference temperature, T_c is the cell temperature (ºC), T is the cell temperature (ºK), K_l is the short-circuit current temperature coefficient (0.0017 A / ºC), H is the cell irradiance (W/m^2),I_{sc} is the module short-circuit current, $E_{go}$is the band gap for silicon. The output of a PV module changes depending on the amount of solar irradiance, the angle of the module with respect to the sun, the temperature of the module and the voltage at which the load is drawing power from the module [10].

B. Wind Energy

Extraction of wind energy in regions having higher standard deviation of wind velocity and low potency is a challenging task [14].To make a model for extraction of wind energy, Weilbull function is generally considered as a good choice [15-16]. Weibull function is given in the equation (4).

$$f(v) = (k/c)\,(v/c)^{k-1}\exp(-(v/c)^{k}) \quad (4)$$

Where
'f' I represents probability density function of wind velocity (PDF),

'v' is velocity of wind (mtr/sec.),
'k' is the shape parameter and
'c' is scale parameter (mtr/sec.).

Values of 'k' and 'c' can be determined using Analytical method [17]. Further, in order to determine velocity of wind in the others hub height following equation may be used (5).

$$U(z)/U(z_r) = (z/z_r.)^{\alpha} \quad (5)$$

U(zr) is the wind velocity in the reference hub height zr(mtr/sec.) and α is location coefficient (= 0.25 [18]).

Therefore, multiplication of power of wind generator at a particular wind velocity with the value of Weibull function [19] represents total power of wind generator.

$$P_W = P_{n-1} + V((P_n - P_{n-1})/(V_n - V_{n-1}))$$
$$\text{in the } V_{n-1} < V < V_n \quad (6)$$

C. Inverter Control

In this control structure as per Fig. 2, there are two control loops; inner control loop and outer control loop. Outer control loop provides a signal which contributes as reference current signal for inner loop control. Point of common coupling (PCC) voltage and current is measured and Park's transformation is applied on it which will provide corresponding V_d, V_q, I_d, and I_q components. V_{dcref} is compared with V_{dc} and error is fed to the V_{dc} control which generates reference current (i_{dref}) for inner loop control. $I_{dref}$is then compared with I_d and error signal is send to Proportional integral (PI) controller in order to ensure that reference is tracked efficiently. As shown in Fig. 2 Pulse width modulation with sine angle memory (SPWM) will give pulses for gate firing of IGBT.

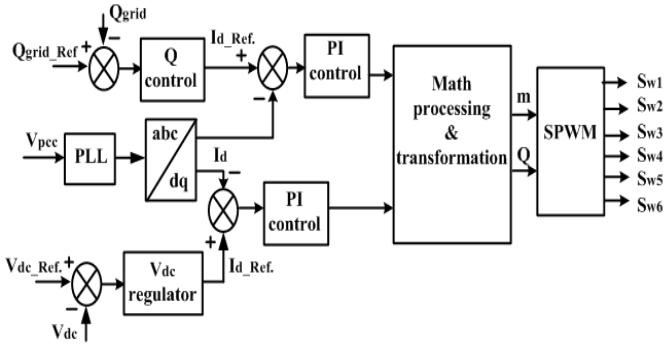

Fig. 2 Control structure for inverter control

D. Grid Side Converter Control

Grid side converter control as shown in fig.3; is designed such that it helps in regulating the voltage level of DC bus capacitor. For the grid-side controller, the d-axis of the rotating reference frame used for d-q transformation is aligned with the positive sequence of grid voltage. Grid side controller mainly contains three sub-components. First is a measuring unit to measure DC voltage (V_{dc}), d and q components of grid current. Second is a DC voltage regulator for outer loop regulation and third is a current regulator for inner current loop.

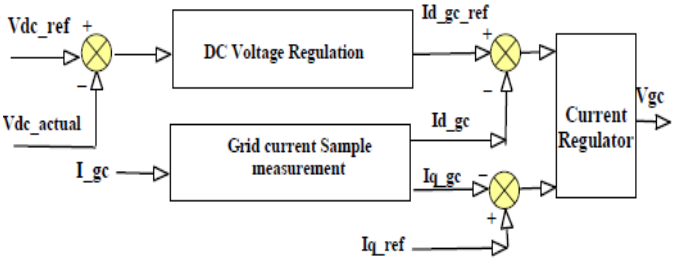

Fig. 3 Grid side converter control block diagram

As depicted in Fig. 3, grid side converter control consists of inner layer and outer layer control loop. In outer loop control error between desired DC bus voltage (V_{dc_ref}) and actual DC bus voltage (V_{dc}) is fed to the DC voltage regulator, which further generates reference current $I_{dgc_ref}$for inner loop control. Similar to outer loop control, error between I_{dgc_ref}andI_{dc} is fed to the current regulator. The voltage of converter C_{grid} is primarily being controlled by its current controller and co-ordinate by feed forward gain as per prediction of C_{grid} output voltage

E. Rotor side Converter Control

A schematic functional control block is shown in fig.4 where rotor excitation voltage signal is derived based on Reference and feedback measured at various locations as shown in the control block.

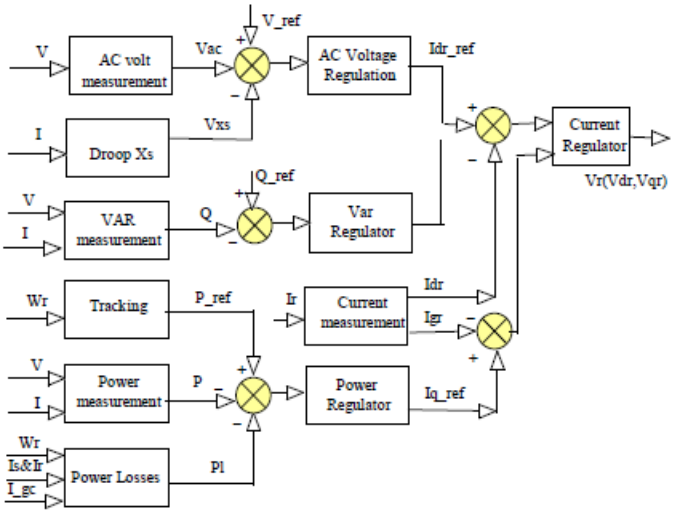

Fig. 4 Rotor converter control block diagram

Rotor side converter control is desired to control the flow of power from wind generator to PCC, while maintaining the voltage level as per grid level. Transfer of power is controlled as per tracking characteristic of the wind generator. Mechanical power corresponding to measured actual turbine speed is considered as reference power of control loop. Reference power thus obtained is compared with the sum of actual measured electrical power at the grid side of wind generator and total power losses including both mechanical and electrical losses.

A properly tuned PI controller reduces the error to close to zero. I_{qr_ref} is the output of PI controller and represents the current required to be injected by the converter C_{rotor} into the rotor. This injected current produces electromagnetic torque T_{em}. I_{qr_ref} is compared with measured I_{qr} and the error thus generated is fed to the PI controller. Voltage V_{qr} which is being generated by C_{rotor}; is the output of PI controller. The current regulator is assisted by feed forward gain predictingV_{qr}.

Reactive power which is being absorbed or generated by C_{rotor} is responsible to maintain voltage level at PCC. Further, C_{rotor} and grid exchanges reactive power through generator and in this process reactive power is absorbed by generator to fulfill the need of power demand of its mutual and leakage inductances; whereas, the excess power is transferred to either C_{rotor} or grid.

In constant Var regulation mode, Var regulator keeps the reactive power constant at PCC. The converter C_{rotor} needs injection of d-axis I_{dr_ref} current which is output of voltage regulator and/or V_{ar} regulator. Similarly actual I_{dr} component as per measurement is being compared with I_{d_ref} and generate error signal as input to final current regulator which is providing output signal V_r which can be decomposed as V_{dr} and V_{qr} as d-axis and q-axis component.

F. Pitch Angle Control

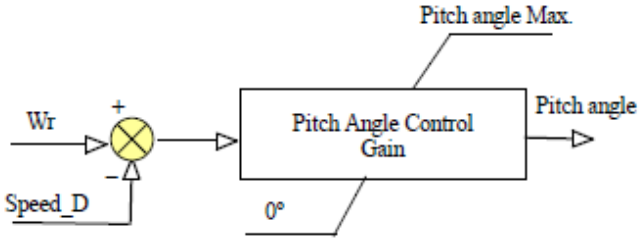

Fig.5 Pitch angle control system

Referring to Fig. 5, the cut-in wind speed is selected so as to keep the rotational speed below the speed at point D for better stability and minimum electromagnetic transients. It is preferable to keep pitch angle aligned to zero line atleast upto turbine speed touches the D speed point of tracking characteristics. It is observed that pitch angle is directly proportional to the speed offset from D point speed.

The pitch angle is kept constant at zero degree until the speed reaches point D speed of the tracking characteristic. Beyond point D the pitch angle is proportional to the speed deviation from point D speed. For electromagnetic transients in power systems the pitch angle control is of less interest. The wind speed should be selected such that the rotational speed is less than the speed at point D.

III. Simulation Results and Discussion

To verify the performance, PV-wind hybrid grid connected (Fig. 1) system is simulated in MATLAB/Simulink and results of simulation are presented in this section. Irradiation is considered uniform at all PV modules at a constant value of 1000 W/m^2. Wind speed is also considered constant at 15 m/hr. Initially local load is considered as 200 kW and at t = 1 sec, load suddenly increased to 300 kW. As depicted in Fig. 6, before t = 1 sec PV system is producing 152 kW and thus operates at MPPT. Whereas wind generator produces 80 kW as per its maximum power generating capacity. Thus total power being generated by PV-wind hybrid system is 232 kW and thus excess power of 32 kW (generated power – power consumed by local load – power losses) is transferred to grid. However after t = 1 sec as local load is increased by 100 kW (total local load = 300 kW), a scenario of power deficit is arrived. In this situation total power generated by PV-wind hybrid system is transferred to the local load. However, still scenario of power deficit occurs. This additional power required by local load is now being supplied by grid (Fig. 6). Reference common DC bus voltage is considered as 720 V

and from Fig. 6 it is evident that actual measured common DC bus voltage (V_{dc}) is almost equal to the reference common DC bus voltage. It is important to note here (Fig. 6) that despite of sudden and large increase in local load at t = 1 sec; there is no dip is noticed in DC bus voltage.

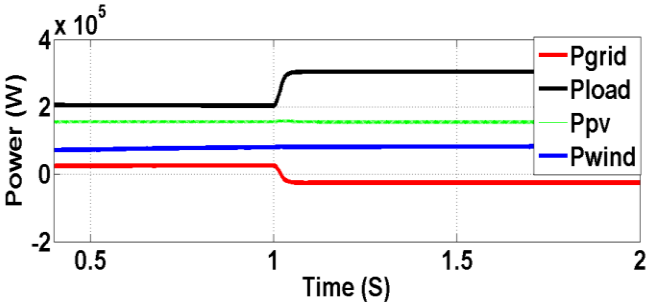

Fig. 6 Power variation with change in local load

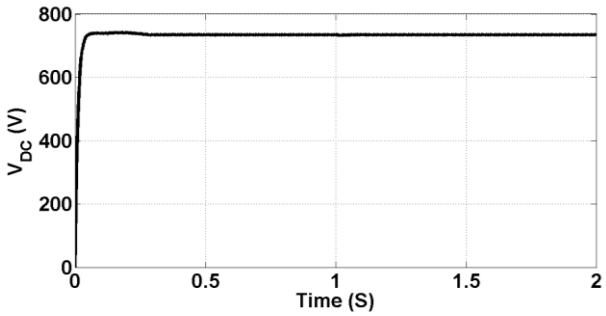

Fig. 7 Variation in common DC bus voltage with time

Local load considered in the proposed system also contains an Induction motor (IM) of 5 kW having a rated RPM of 1233. As shown in Fig. 8 before t = 1 sec IM is running at its rated RPM. However at t = 1 sec as local load is increased to 300 kW, a dip in IM RPM is observed. Further, as deficit power is being supplied by grid, so again IM is able to operate at its rated RPM.

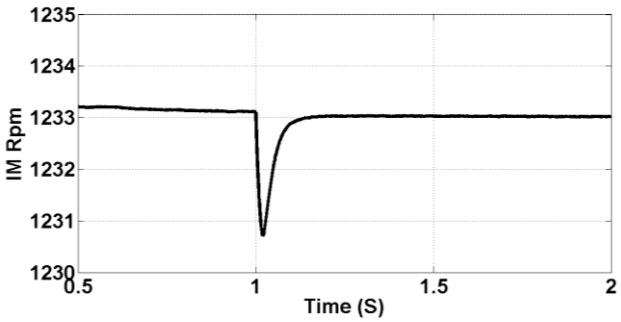

Fig. 8Variation in RPM of IM with time

Fig. 9 and Fig. 10 represent 3-phase voltage at PCC and utility grid. Proposed PV-wind hybrid system with its dedicated control structure is able to maintain system's voltage as per voltage level at PCC despite of variation in demand of power (Fig. 9).

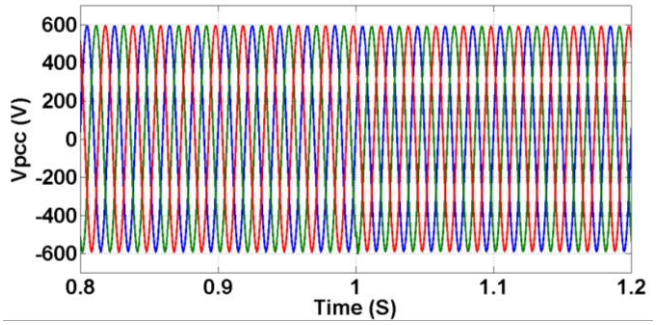

Fig. 9 Variation in voltage at PCC with time (Volt)

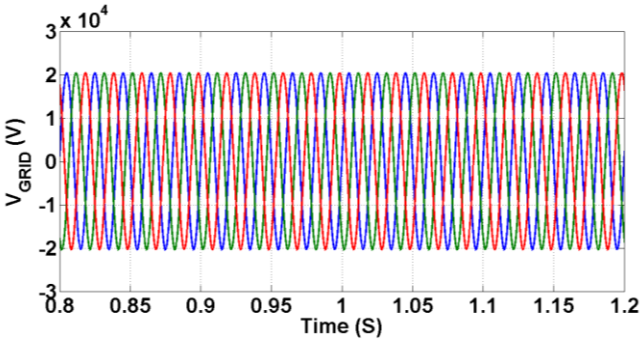

Fig. 10Variation in grid voltage with time (Volt)

IV. Conclusion

In this paper, a PV-wind hybrid grid connected system is proposed. Single stage PV system is considered and maximum extraction of PV power is ensured through inverter control. Extraction of wind energy is governed by pre-specified tracking characteristics of wind generator. Inverter control is taking care of current injection from PV generator to PCC. Further, grid side converter and rotor control is responsible for transfer of energy from wind generator to grid terminals. Proposed system is simulated in MATLAB/Simulink considering sudden change in local load. Designed system is able to meet the demand of local load while maintaining the voltage level at PCC without support of ESD.

References

[1]. European Commission, EU Energy Trends to 2030, Luxembourg, Publications Office of the European Union, accessedon:http://ec.europa.eu/energy/observatory/trends_2030/, 2010.

[2]. E. Koutroulis, K. Kalaitzakis, N. C. Voulgaris, "Development of a microcontroller-based, photovoltaic maximum power point tracking control system". IEEE Transactions Power Electronics, vol. 16, No 1, pp. 46-54, 2001.

[3]. I. Houssamo, F. Locment, M. Sechilariu, "Maximum power tracking for photovoltaic power system: Development and experimental comparison of two algorithms". Renewable Energy, vol. 35, No 10, pp. 2381-2387, 2010.

[4]. I. H. Altasa, A. M. Sharaf, "A novel maximum power fuzzy logic controller for photovoltaic solar energy systems". Renewable Energy, vol. 33, No 3, pp. 388-399, 2008.

[5]. Syafaruddin, E. Karatepe, T. Hiyama, "Polar coordinated fuzzy controller based real-time maximum-power point control of photovoltaic system". Renewable Energy, vol. 34, no 12, pp. 2597-2606, 2009.

[6]. C. Larbes, S. M. A. Cheikh, T. Obeidi, A. Zerguerras, "Genetic algorithms optimized fuzzy logic control for the maximum power point tracking in photovoltaic system". Renewable Energy, vol. 34, No 10, pp. 2093-2100, 2009.

[7]. T. Tafticht, K. Agbossou, M. L. Doumbia, A. Chériti, "An improved maximum power point tracking method for photovoltaic systems". Renewable Energy, vol. 33, No 7, pp. 1508-1516, 2008.

[8]. A. Chaouachi, R. M. Kamel, K. Nagasaka, "A novel multi-model neuro-fuzzy-based MPPT for three-phase grid-connected photovoltaic system". Solar Energy 2010;84(12):2219-2229.

[9]. N. Hamrouni, M. Jraidi, A. Chérif, "New control strategy for 2-stage grid-connected photovoltaic power system". Renewable Energy, vol. 33, no 10 pp. 2212-2221, 2008.

[10]. H. Mark, "Solar Electric Systems for Africa," Agrotech and Commonwealth Science Council, 2005.

[11]. M. H. Rashid, Power Electronics, India: Pentice Hall, 2005.

[12]. Muralidhar Killi, Samanta S., "Modified Perturb and Observe MPPT Algorithm for Drift Avoidance in Photovoltaic Systems", IEEE Transactions on Industrial Electronics, Vol. PP, Issue 99, February 2015.

[13]. Yohan Hong,Pham S.N., Taegeun Yoo, Kookbyung Chae, Kwang-Hyun Baek, Yong Sin Kim, "Efficient Maximum Power Point Tracking for a Distributed PV System under Rapidly Changing Environmental Conditions", IEEE Transactions on Power Electronics, Vol. 30, Issue 8, pp. 4209-4218, March 2015.

[14]. J. L. Acosta, A. J. Collin, B. Hayes, and S. Z. Djokic, "Micro and Small-scale Wind Generation in Urban Distribution Networks," presented at the 7th Mediterranean Conference and Exhibition on Power Generation, Transmission, Distribution and Energy Conversion, Agia Napa, Cyprus, 2010, pp. 1–9.

[15]. W.-H. Shi and J. Chen, "Reliability Assessment of Interconnected Generation Systems Based on Hourly Wind Speed Probability Model," in SciVerse Science Direct, Chengdu, China, 2011, vol. 12, pp. 819–827.

[16]. K. M. Nor, M. Shaaban, and H. A. Rahman, "Feasibility assessment of wind energy resources in Malaysia based on NWP models," Renewable Energy, vol. 62, pp. 147–154, 2014.

[17]. D. Saeidi, M. Mirhosseini, A. Sedaghat, and A. Mostafaeipour, "Feasibility study of wind energy potential in two provinces of Iran: North and South Khorasan," Renewable and Sustainable Energy Reviews, vol. 15, pp. 3558–3569, 2011.

[18]. A. Mostafaeipour, "Economic evaluation of small wind turbine utilization in Kerman, Iran," Energy Conversion and Management, vol. 73, pp. 214–225, 2013.

[19]. B. O. Bilal, M. Ndongo, C. M. F. Kebe, V. Sambou, and P. A. Ndiaye, "Feasibility study of wind energy potential for electricity generation in the northwestern coast of Senegal," in Energy Procedia, 2013, vol. 36, pp. 1119–1129.